Nonlinear Thickness and Grain Size Effects on the Thermal Conductivity of $CuFeSe_2$ Thin Films

P. C. Lee,[1,2,3,*] M. N. Ou,[3] Z. W. Zhong,[3] J. Y. Luo,[3] M. K. Wu,[3] K. C. Chen,[3] and Y. Y. Chen[3,†]

[1]*Department of Engineering and System Science, National TsingHua University, Hsinchu, Republic of China*
[2]*Nano Science and Technology Program, Taiwan International Graduate Program, Academia Sinica, Taipei, Republic of China*
[3]*Institute of Physics, Academia Sinica, Taipei, Republic of China*

(Received May 7, 2012)

A crucial issue in realizing the applications of high-density semiconductor devices is no more than heat dissipation, especially in the direction perpendicular to the substrate. For the past decades, crystallization effects on thermal conductivity have been intensively studied, whereas the quantitative analysis on this aspect is rare. In this study, a series of $CuFeSe_2$ thin films with grain sizes 20–40 nm controlled by the thickness were fabricated for the quantitative study of the grain size effect on the thermal conductivity perpendicular to the subtract. The results reveal that larger grain sizes have higher thermal conductivity and the trend agreed well with the simplified theory of the phonon-grain boundary interaction. From the data of electrical conductivity and the Wiedemann-Franz law, the thermal conductivity is mainly contributed by the lattice thermal conductivity, and is nonlinearly dependent on the grain size and the thickness of the films. In addition, the $\sim 2.6\times10^{-8}$ K-m^2/W film-substrate interfacial thermal resistance (comparable to that of 200 nm films) is also a non-negligible factor and has to be taken into account.

DOI: 10.6122/CJP.51.166 PACS numbers: 65.40.-b, 68.55.ag, 68.60.Dv

$CuFeSe_2$ is a type I-III-VI_2 semiconductor and is considered to be a small band gap photoelectric material with a direct band gap of 0.16 eV [1]. It has a tetragonal structure (space group$P$-42c) with lattice constants $a = 5.53$ Å and $c = 11.049$ Å [1]. To date, only a few research articles focused on this material have been reported [1–4].

For the development of high density integrated circuits in semiconductor products, rapid power dissipation is an inescapable requirement. Since thin films are the main components of electronic devices, their thermal properties have been extensively studied and reported in the literature [5–8]. In general, thin films are grown or deposited on substrates. Therefore, where power dissipation is considered, the thermal conductivity of the film as well as the thermal boundary resistance at the interface between the thin film and the substrate has to be taken into account. In the earlier reports made by the differential 3ω measurement technique, the thermal conductivity was considered to be identical for all the film specimens having different thicknesses [5, 9, 10]. Based on this assumption, the thermal

*Electronic address: iamplex@phys.sinica.edu.tw
†Electronic address: cheny2@phys.sinica.edu.tw

resistance of the film is linearly dependent on the film thickness, and the intercept of the linear fit is the boundary resistance of the interface. In this study, a series of high-quality $CuFeSe_2$ thin films with various grain sizes ranging from 20–40 nm (corresponding to thickness 200 to 800 nm) were prepared and studied to examine the thermal conductivity and thermal boundary resistance between the thin film and substrate. The $CuFeSe_2$ thin films grown by pulse laser deposition (PLD) having different grain size were controlled by the thickness of film deposition. The thin films were grown on silicon substrates, and their structure and grain size characterized by X-ray diffraction. The temperature dependence of the cross-plane thermal conductivities of the thin films was measured using the differential 3ω technique. To obtain the thermal boundary resistance between the thin films and the silicon substrate, the thermal resistance was plotted against the film thickness and the results fitted to a curve. The thermal boundary resistance between the thin films and the silicon substrate is defined as the intercept on the curve at zero thickness. The intrinsic thermal conductivity of each thin film was obtained after subtraction of the thermal boundary resistance.

The thin films were grown by PLD using a target to give the following composition, Cu:Fe:Se = 1:1:2. The target of size 25 mm in diameter by 8 mm in thickness was sintered at 600–700 °C in a vacuum. The target was then mechanically polished prior to each deposition process for the purpose of consistency and reproducibility for successive depositions. Thin films were deposited by a KrF excimer laser with $\lambda = 248$ nm and a power density of 5–6 J/cm^2 (Lambda Physik LPX Pro) at a pulse frequency of 5 Hz in a vacuum of 10^{-5} Torr. The distance between the target and the substrate was set to around 4.7 cm. Thin films were deposited on 12×12 mm^2 pre-cleaned Si (1 0 0) substrates having a SiO_2 insulation layer with a thickness of 400 nm at a temperature of 250 °C.

The obtained $CuFeSe_2$ films were characterized by X-ray diffraction using a PANalytical X'Pert PRO MPD system equipped with a copper anode tube as the source and a multi-channel X'Celerator as the detector (Fig. 1). The films were found to have a tetragonal structure, as confirmed by the diffraction data shown in Fig. 1, and a highly aligned crystalline structure with a preferred orientation in the (h 0 0) plane, as is evident from the (100), (200), and (300) diffraction peaks. This implies that the thin films have an a-b plane perpendicular to the silicon substrate surface. However, for thicker films, a small peak of $CuFeSe_2$ (112) starts to grow in the 400 nm film, and a minor phase of Cu_2Se (111) is observed in the 600 and 800 nm films. It is clearly observed that the thicker films have a broader line width than the thinner films (the inset of Fig. 2 (a)). The wider FWHM (full width at half maximum) of the thin film is an indication of the smaller grain size and/or a higher strain in the sample. By applying Sherrer's equation, the grain sizes of the thin films were calculated; the grain size shows an exponential dependence on film thickness (Figure 2 (a)). Since the thermal resistivity is mainly determined by the grain size and grain boundary, this results in a nonlinear thickness dependence of the thermal resistance.

To examine the degree of preferred orientation (1 0 0) and crystallization in the films, the mosaic spread of the rocking curves (1 0 0) of the 200, 600, and 800 nm films at $\theta = 16.104°$ were measured and analyzed using a PANalytical X'Pert PRO MRD system. It is clear from the results that the 600 and 800 nm films have a broader width than the

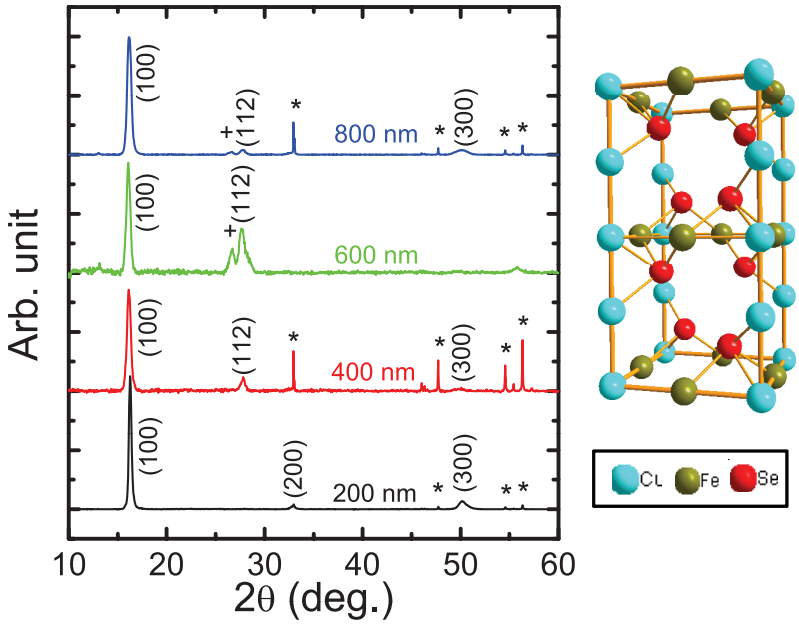

FIG. 1: X-ray diffraction patterns for films of various thicknesses. The (100), (200), and (300) planes are clearly observed in the 200 and 400 nm thick films. Asterisks (*) represents the peak of the SiO_2 substrate. Daggers (+) represents the minor phase Cu_2Se (111) peak in the 600 and 800 nm thick films. The tetragonal structure of $CuFeSe_2$ is shown to the right of the X-ray diffraction patterns.

200 nm sample (Fig. 2 (b)). Obviously, the thicker $CuFeSe_2$ film has a (1 0 0) preferred orientation and a crystallinity that is poorer than that of the 200 nm film. This consequence is strongly correlated to the lower thermal conductivity in the thicker films, which will be discussed below.

The in-plane electrical resistivity was measured using the four probe method with a Quantum Design PPMS. Figure 3 shows the temperature dependent electrical resistivity of the 200, 600, and 800 nm film samples; the data implies that the thin films undergo semiconductor-like behavior. The activation energy can be estimated using the formula

$$R = R_0 e^{(E_a/k_B T)}, \tag{1}$$

where R is the resistivity, E_a is the activation energy, and k_B is Boltzmann's constant [11]. The inset of Fig. 3 shows the temperature dependent activation energy of the $CuFeSe_2$ thin films, which is the differential of the $\ln R$ versus $1/T$ plot. The calculated activation energy of the $CuFeSe_2$ thin films is 0.16 eV for the 200 nm film and 0.1 eV for the 600 and 800 nm films. These results correspond well with the band gap of $CuFeSe_2$ (0.16 eV) reported in the literature [1].

The cross-plane thermal conductivity of the films was measured using the differential 3ω technique with two microprobes [6, 8, 12–14]. One of the two microprobes was placed on the deposited thin film and the other one placed directly on the silicon substrate. With these

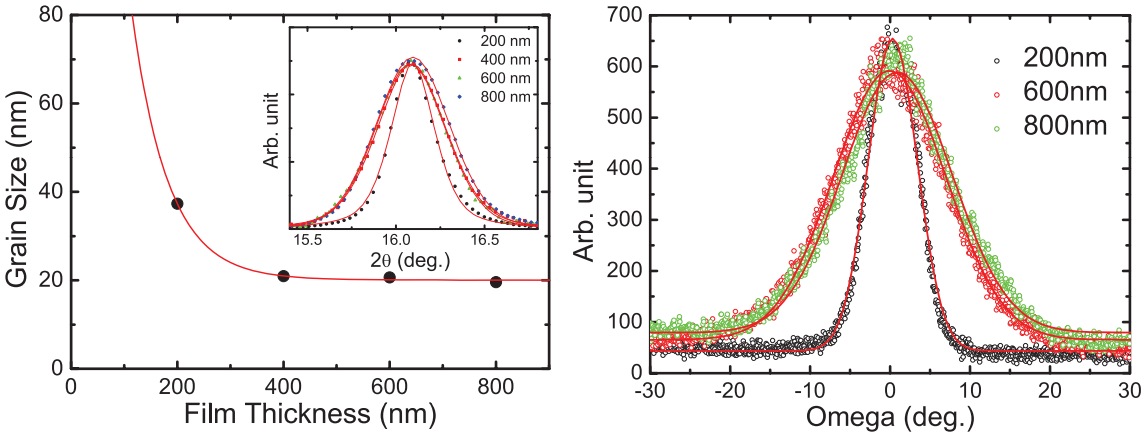

FIG. 2: (a) The thickness dependence of grain size in $CuFeSe_2$ thin film samples. The larger grain size is evident in the thinner samples. Inset: Films of thinner thickness exhibit a narrower (100) plane diffraction peak width. (b) The rocking curve profile for 200, 600, and 800 nm thickness films: the thinner films exhibit better preferred orientation.

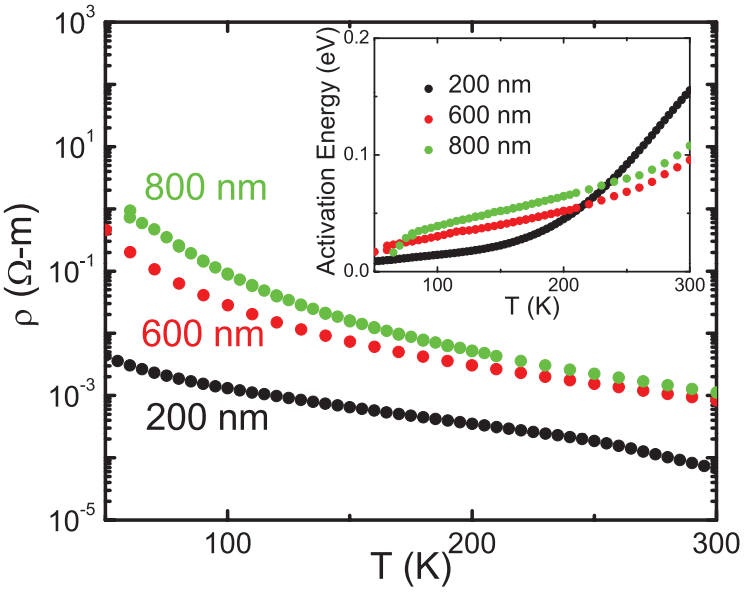

FIG. 3: The temperature dependence of the electrical resistivity of the 200, 600, and 800 nm films. All thin films studied demonstrate semiconducting-like behavior. Inset: the temperature dependence of the activation energy for 200, 400, and 800 nm thickness films.

two microprobes, the temperature drop across the thin film was measured, and the thermal conductivity was derived afterwards (the schematic diagram of the specimen configuration is shown in Fig. 4). To prevent a direct electrical contact between the microprobes and the film/substrate, a 300 nm SiN_x insulation layer with a high thermal conductivity was pre-

deposited by PECVD (plasma-enhanced chemical vapor deposition) onto the film/substrate. Gold strips of 150 nm in thickness, 4 μm in width, and 1.5 mm in length were deposited as microprobes onto the SiN_x insulation layer using photolithography. The microprobes were powered by an AC power P at frequency ω, and the resulting third-harmonic voltage was read using a lock-in amplifier. The 3ω signals on both the thin film and reference were converted to an AC temperature variation amplitude. The difference between the two microprobes corresponds to the temperature drop ΔT across the $CuFeSe_2$ thin film, which is used to calculate the cross-plane thermal conductance by $P/\Delta T$.

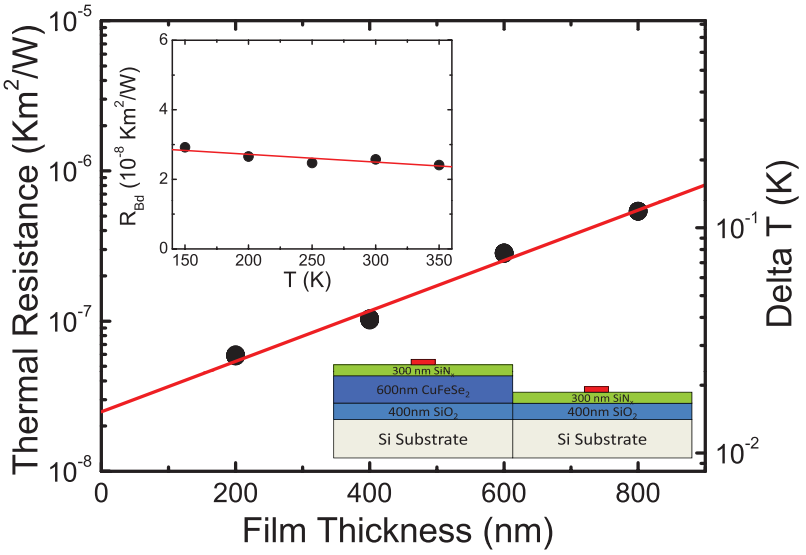

FIG. 4: The normalized thermal resistance of different thickness specimens at room temperature. The solid line shows the exponential fitting of the measurement data and the intercept T_0 indicates the temperature drop across the interfaces. Inset: The temperature dependence of the thermal boundary resistance R_{Bd} of interfaces, and the schematic diagram of the specimen configuration for thermal conductivity measurements.

The measurement frequencies ranged from 10 to 1000 Hz with $\sim$ 5 mW applied power. The normalized thermal resistance and the temperature drop ΔT, caused by the thin film and boundary of the various thickness films are shown in Figure 4. It is clearly observed that the thermal resistance of this series of thin film samples is exponentially dependent on the film thickness, which does not fit in with the normal situation (a linear dependence). This behavior could be attributed to the structural disorder in the thick films, as revealed by the X-ray diffraction data, i.e., thinner films have structures with better crystallinity. The temperature drop was fitted using the equation $\Delta T = \Delta T_0 \exp(a * t)$ for each measurement temperature: t represents the film thickness, and ΔT_0 represents the temperature drop across the boundary. The temperature dependencies of the thermal boundary resistance R_{Bd} $(= \Delta T_0/P)$ at the interface calculated from the intercept of the fitting plots were 2.9×10^{-8} and 2.6×10^{-8} K-m^2/W at 150 and 300 K, respectively. The inset of Fig. 4 shows that R_{Bd} decreases linearly with increasing temperature, which behaves similar to

that previously reported [15]. Applying this result to all the thin film samples, the intrinsic thermal conductivity for each film was obtained and plotted in Fig. 5. Principally, the cross-plane thermal conductivity increases weakly with increasing temperature. At 300 K, the thermal conductivity of the 200, 400, 600, and 800 nm films are 3.4, 3.2, 2.1, and 1.5 W/m-K, respectively. According to the Wiedemann-Franz law, the thermal conductivity contributed by the conducting electrons k_E can be calculated from the electrical resistivity ρ by

$$k_E = L_0 T/\rho \,, \tag{2}$$

where L_0 is the Lorentz number. The inset (a) of Figure 5 shows the main contribution of the thermal conductivity in the 200 nm film, which was mainly attributed to the lattice phonons; only 3% of the thermal conductivity was contributed by the conducting electrons. The inset (b) of Figure 5 shows the grain size dependence of thermal conductivity. In situations where the sample effective grain sizes (d_s) are smaller than the phonon mean free path (l_t), the simplified theory of phonon thermal conductivity as a function of grain boundary can be expressed as [16–19]

$$K_L = \left(\frac{2k_S}{3}\right)\left[\left(\frac{3d_S}{l_t}\right)\left(\frac{k_S}{2k_0}\right)\right]^{1/4}, \tag{3}$$

where K_L is the phonon thermal conductivity, k_s is the phonon thermal conductivity of crystals having negligible phonon boundary scattering in large grain size, k_0 is the phonon thermal conductivity in the absence of alloy scattering, and d_s is the grain size. The solid line and dashed line shown in inset (b) of Figure 5 are the theoretical simulation with $k_0 = 20$ W/m-K and $k_s = 10$ W/m-K for phonon mean free paths equal to 100 and 300 nm, respectively; the measurement results are located well within the theoretical simulations. This result demonstrates that the quality of the crystallization can dramatically affect the value of the thermal conductivity.

The thermal conductivity of a highly crystalline $CuFeSe_2$ thin film deposited on a silicon oxide substrate was studied. The temperature dependent thermal boundary resistivity was extracted, and the exact thermal conductivity of the thin film was obtained after correction for the thermal boundary. The thicker films were found to have lower thermal conductivities due to the smaller grain size and poor preferred orientation. The magnitude of the thermal conductivity (3.4 W/m-K) of the 200 nm thick sample was about two times that of the thermal conductivity (1.5 W/m-K) of the 800 nm films at 300 K. The lower thermal conductivity in the thicker films is attributed to the greater amount of phonon scattering at the grain boundaries as compared to thinner films. The film thickness dependence on the crystallization and grain size were confirmed by the X-ray diffraction data. Essentially, the thermal conductivity of thin films is contributed by lattice phonons. In this report, the thermal resistance of the interface boundaries in $CuFeSe_2$-SiN_x was estimated to be 2.6×10^{-8} K-m^2/W at room temperature, which is approximately equal to that of a $CuFeSe_2$ film of 200 nm thickness. In conclusion, the correlation among thermal conductivity, crystallization, and film thickness is represented in the series of thin films studied.

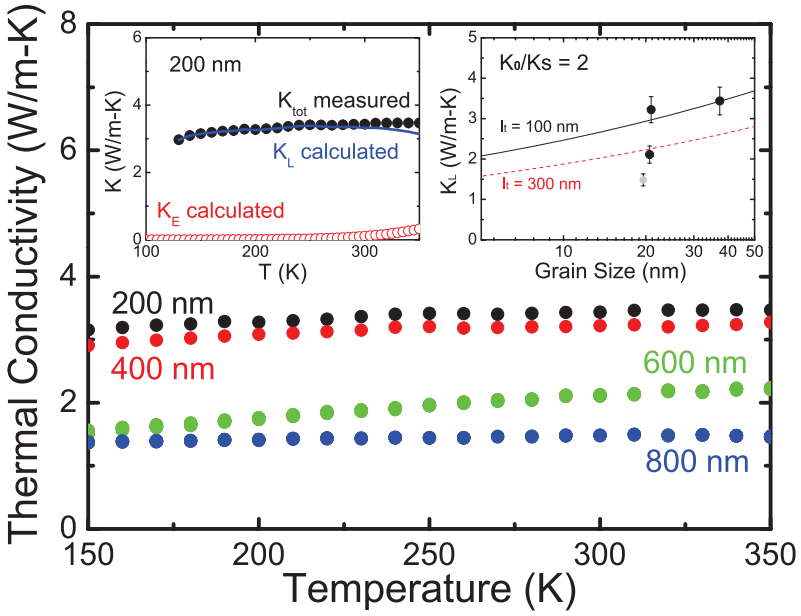

FIG. 5: The thermal conductivity of $CuFeSe_2$ films with different thicknesses for T =150–350 K . Inset (a): the thermal conductivities of the lattice phonons and conducting electrons derived from electrical resistivity data. Inset (b): the thermal conductivities of films with different grain sizes. The theoretical simulations for phonon mean free paths of 100 and 300 nm are represented by the solid and dashed lines, respectively.

Acknowledgements

We would like to thank NanoCore, the Core Facilities from Nanoscience and Nanotechnology at Academia Sinica in Taiwan, and the Micro Optics Electrical Laboratory (National Central University, Taiwan) for their technical support. We would also like to thank Miss I Chen Tsai for her help with manuscript preparation. The work was supported by the Academia Sinica and National Science Council, Republic of China, under Grant No. NSC100-2112-M-001-019-MY3.

References

[1] N. Hamdadou, M. Morsli, A. Khelil, and J. C. Bernede, J. Phys. D Appl. Phys. **39**, 1042 (2006).
[2] F. Gonzalez-Jimenez *et al.*, Physica B **261**, 987 (1999).
[3] Q. Y. Lu *et al.*, J. Cryst. Growth **217**, 271 (2000).
[4] J. Lamazares, *et al.*, J. Magn. Magn. Mater. **104**, 997 (1992).
[5] D. W. Song *et al.*, Appl. Phys. Lett. **84**, 1883 (2004).
[6] H. Tong *et al.*, Appl. Phys. Lett, **97** (2010).
[7] B. Yang, J. L. Liu, K. L. Wang, and G. Chen, Appl. Phys. Lett. **80**, 1758 (2002).
[8] D. G. Cahill, M. Katiyar, and J. R. Abelson, Phys. Rev. B **50**, 6077 (1994).

[9] E. S. Landry and A. J. H. McGaughey, Phys. Rev. B **80** (2009).
[10] P. E. Hopkins, L. M. Phinney, J. R. Serrano, and T. E. Beechem, Phys. Rev. B **82** (2010).
[11] B. J. Lokhande, P. S. Patil, and M. D. Uplane, Mater. Lett. **57**, 573 (2002).
[12] D. G. Cahill, Rev. Sci. Instrum. **73**, 3701 (2002).
[13] T. Borca-Tasciuc, A. R. Kumar, and G. Chen, Rev. Sci. Instrum. **72**, 2139 (2001).
[14] B. N. Pantha *et al.*, Appl. Phys. Lett. **92** (2008).
[15] P. E. Hopkins, R. N. Salaway, R. J. Stevens, and P. M. Norris, Int. J. Thermophys. **28**, 947 (2007).
[16] H. J. Goldsmid and A. W. Penn, Phys. Lett. A **A 27**, 523 (1968).
[17] J. W. Sharp and H. J. Goldsmid, in *Thermoelectrics, 1999. Eighteenth International Conference on*, (IEEE, 2000), p. 709.
[18] M. Takashiri *et al.*, J. Appl. Phys. **104** (2008).
[19] D. M. Rowe *et al.*, *CRC Handbook of Thermoelectrics*, ed. D. M. Rowe (CRC, Boca Raton, FL, 1995).